Mechanical properties of phase-pure bulk Ta_4AlC_3 prepared by spark plasma sintering and subsequent heat treatment

Guobing Ying[1,*], Cong Hu[1], Lu Liu[1], Cheng Sun[1], Dong Wen[2], Jianfeng Zhang[1], Yongting Zheng[3], Minghui Wang[1], Chen Zhang[1], Xiang Wang[2], Cheng Wang[1]

[1]*Department of Materials Science and Engineering, College of Mechanics and Materials, Hohai University, Nanjing, 211100, China*

[2]*Key Laboratory of Superlight Materials & Surface Technology (Harbin Engineering University), Ministry of Education, Harbin 150001, China*

[3]*Center for Composite Materials and Structures, Harbin Institute of Technology, Harbin 15001, China*

Abstract

High-purity and bulk Ta_4AlC_3 ceramics were successfully fabricated by spark plasma sintering (SPS) and subsequent heat treatment, using the raw materials including TaC and Ta_2AlC powders. These raw materials were first synthesized by self-propagation high temperature synthesis from elements tantalum, aluminium and carbon black powders, followed by pressure-less sintering. The as-fabricated bulk Ta_4AlC_3 was relatively stable when subjected to heat treatment at elevated temperature of 1500 °C. Moreover, prolonging the heat treatment time resulted in bigger grain sizes and higher densities of the Ta_4AlC_3. The flexural strength and the fracture toughness of the Ta_4AlC_3 fabricated by SPS were found to be 411 MPa and 7.11 MPa·m^{1/2}, respectively. After the heat treatment at 1500 °C for 8 h, the flexural strength and the fracture toughness of the Ta_4AlC_3 could reach 709 MPa and 9.23 MPa·m^{1/2}, respectively. The special structural characteristics of the ternary ceramics and the increase of density after the heat treatment are the main reasons for the variation in mechanical properties of ternary ceramics.

Keywords: Ta_4AlC_3, spark plasma sintering, heat treatment, microstructure, mechanical properties

I. Introduction

The $M_{n+1}AX_n$ or MAX phases, as a series of early transition-metal carbides and nitrides where n = 1, 2, or 3, M is an early transition metal, A is an A-group element (mostly groups 13 and 14), and X is C and/or N, consisting of hexagonal crystals, nanolayered microstructure and unique machinable phases with an unusual combination of both metallic and ceramic properties [1]. Since the discovery of several 211 phases (e.g. Ti_2AlC [2], then referred to as "H-phases") and two 312 phases (i.e. Ti_3SiC_2 [3] and Ti_3GeC_2 [4]) by Nowotny's group [5] in the 1960s, more than 150 MAX compositions have been developed by the researchers [6]. Among them, Barsoum's group [7] started their related work in 1996 and then presented the most remark-

able study in their more than 300 literature reports. In addition, the well-known scientist Zhou and his group [8] have devoted extensive research efforts after their first report on *in situ* hot pressing/solid-liquid reaction of Ti_3SiC_2 ceramics in 1998. Moreover, the well-known group of Eklund [9] at Linkoping University has also been attempting related studies and most of them involve the characterization and properties of the MAX films [10].

The MAX phases have attracted significant research attention not only because of the unusual combination of both metallic and ceramic properties, but also for other significant extraordinary properties [11–17]. In general, among them, M [12,14], A [11,13] and/or X [15,16] site solutions, nanolayered behaviour [18,19] and selected etched precursors for MXenes [20–23] make MAX phases significantly different from other materials. To the best of our knowledge, more than 50

*Corresponding author: tel: +86 25 58099150,
e-mail: *yinggb2010@126.com, yinggb001@hhu.edu.cn*

MAX solutions with different M, A and X compositions have been reported till date [6]. Moreover, the nanolayered behaviour [24] always refers to relatively soft [25], damage tolerant [26] and plastic at high temperatures [27]. Special layered structures usually have basic 211, 312 and 413 $P6_3/mmc$ lattices with M-X octahedra interleaved with layers of A elements. In contrast, other hybrid structures (e.g. 523, 725) can be described as a combination of the basic conventional MAX phases [6]. Another typical deformation refers to the compression of nanolayered MAX by ripplocation nucleation, and that in turn leads to kink-band formation, which was disclosed by Barsoum and Tucker [28]. The ripplocation is obviously different from dislocation slip and deformation twinning. Moreover, MAX phases are also common for two-dimensional MXenes and they will be progressively more extensive and significant due to the application prospects of new MXene with composition variations and property tuning [29–34].

Ta_4AlC_3, a member of the family of MAX phases, was first reported by Lin *et al.* [35] in 2006 as bulk Ta_4AlC_3 and then soon confirmed by Manoun *et al.* [36]. The bulk modulus of Ta_4AlC_3 was calculated to be 261 GPa [37] and Ta_4AlC_3, so far, consists of the highest M for any single-phase and non-solid solution MAX (comparable tungsten solutions: $(W_{2/3}Sc_{1/3})_2AlC$ and $(W_{2/3}Y_{1/3})_2AlC)$ [38,39]. Synthesis of bulk Ta_4AlC_3 was first reported by Hu *et al.* [40] in 2007 by hotpressing (HP). Very recently, Griseri *et al.* [41] fabricated bulk and high phase purity Ta_4AlC_3 MAX phase ceramics by HP and spark plasma sintering (SPS). However, these reports on Ta_4AlC_3 still have some challenging and missing research areas to identify. Firstly, X-ray diffraction (XRD) pattern of the Ta_4AlC_3 sample needs to be determined. Eklund *et al.* [9] reported the details about d and 2θ values, and calculated and experimentally normalized relative intensities for allowed hkl peaks of Ta_4AlC_3 where the $(hkl) = (106)$ with $I_{calculated} = I_{observed} = 100\%$ at 2θ of ~23.17°. However, Hu *et al.* [40] showed the $(hkl) = (105)$ with $I_{calculated} = I_{observed} = 100\%$ at 2θ of ~38.60° and (106) at 2θ of ~40.70°. Moreover, in 2019 Griseri *et al.* [41] showed the $(hkl) = (002)$ with $I_{calculated} = I_{observed} = 100\%$ at 2θ of ~7.70° or the $(hkl) = (0010)$ with $I_{observed} = 100\%$ at 2θ of ~38.00°, which corresponds to (106) at 2θ of ~40.70°. Secondly, Ta-Al-C and Ta_2H-Al-C powders mixtures were previously prepared into dense polycrystalline samples of Ta_2AlC and Ta_4AlC_3 by SPS or HP. During the processing, the solid-liquid reaction resulted in the melting of Al at elevated temperature. Ta-Al intermetallics, Al_2O_3 and TaC are frequently found in synthesized Ta_4AlC_3. Griseri *et al.* [41] synthesized α-Ta_4AlC_3 with high-purity of 99% (with Al_2O_3) by HP at 1500 °C for 30 min at 30 MPa and the β-Ta_4AlC_3 allotrope (80% α-Ta_4AlC_3 and 20% β-Ta_4AlC_3, with Ta-Al intermetallic and Al_2O_3) was observed in the samples produced by SPS. Formation of dense, high-purity and bulk α-Ta_4AlC_3 by SPS remains a challenging task.

Thirdly, report by Griseri *et al.* in 2019 [41] showed the XRD pattern and α-β-Ta_4AlC_3 bulk samples prepared by SPS, which exhibited thermal decomposition and existence of pores. The result revealed only a small difference in phase composition and 2θ values between α-Ta_4AlC_3 and β-Ta_4AlC_3 samples based on the XRD patterns. Thus, additional investigation and clarification of XRD results are required.

The main objective of this study was to synthesize high-purity α-Ta_4AlC_3 by SPS involving a series of strategies and resolve the dispute encountered in previous studies related to Ta_4AlC_3. Dense and bulk Ta_4AlC_3 ceramics were synthesized by *in situ* SPS/solid-solid reaction using TaC and sintered Ta_2AlC as raw materials. Furthermore, the conflicts on the XRD pattern of α-Ta_4AlC_3 were also resolved. The effect of heat treatment on the microstructures and mechanical properties of bulk Ta_4AlC_3 ceramics prepared by SPS was also investigated.

II. Experimental

Commercial powders of tantalum (99.99 wt.%, ~45 μm, Ningxia Orient Tantalum Industry Co. Ltd, Ningxia, China), aluminium (99.7 wt.%, ~29 μm, China Northeast Light Alloy Co. Harbin, China), tantalum carbide (99.5 wt.%, >2 μm, Ningxia Orient Tantalum Industry Co. Ltd, Ningxia, China) and carbon black (99.0 wt.%, 18 nm, Tianjin Yiborui Chemical Co. Ltd.) were used as raw materials. The tantalum, aluminium and carbon black powders with a molar ratio of Ta : Al : C = 2 : 1.4 : 1 were wet-mixed in absolute ethanol using a planetary ball mill for 15 h. Stainless steel balls were used as the mixing medium. The milled mixture was dried in a rotating evaporator and compacted uniaxially in a steel die under a pressure of 50 MPa. The as-obtained green compacts with a dimension of $\varnothing 50 \times 10$ mm were sintered by self-propagation high temperature synthesis (SHS) in air, which resulted in the formation of Ta_2AlC. Related details could be found elsewhere [42]. The Ta_2AlC samples prepared via SHS were ground with SiC emery paper to remove the outer surface and they were crushed into powders. The Ta_2AlC powders were washed with hydrochloric acid (HCl, 1 mol/l). The washed Ta_2AlC powders were dried and sieved passed through a sieve size of ~45 μm. For comparative analysis, these powders were also pressureless sintered (PLS) in tube furnace at 1500 °C for 1 h under a flow of pure argon (99.99%) and then crushed into powders with the particle size of ~45 μm, thus phase pure Ta_2AlC powders could be obtained.

The phase pure Ta_2AlC (~45 μm) and TaC powders with molar ratios of Ta_2AlC : TaC = 1 : 0.8, 1 : 1.2, 1 : 1.6 and 1 : 1.8 were considered for the fabrication of Ta_4AlC_3. The mixed powders were placed into a BN-coated graphite die and cold pressed uniaxially under 20 MPa. Further on, the green body together with the die was heated to 1500 °C in an Ar atmosphere at a heating

rate of 80 °C/min, and hot pressed at this temperature for 10 min under a pressure of 30 MPa using SPS.

The phase composition of the pressure-less sintered powders, SPS sintered material and heat-treated material were tested by XRD using a X-ray diffractometer operated with Cu Kα radiation (Rigaku Smart lab, Rigaku Corporation, Tokyo, Japan). The refinements of XRD patterns were performed by Rietveld method using the Fullprof [43]. Microstructures of the samples were observed by scanning electron microscopy (SEM, S-4800, Hitachi, Tokyo, Japan). The densities of the sintered and heat-treated samples were measured by the Archimedes method. The Vickers hardness was determined under a load of 10 N with a fixed contact time of 15 s using a hardness tester. Flexural strength was determined via three-point bending of parallelepipeds with a dimension of 3 mm × 4 mm × 36 mm, using a 30 mm span and a crosshead speed of 0.5 mm/min. Fracture toughness was determined by the single-edge-notched beam technique. Moreover, the parallelepipeds with dimensions of 2 mm × 4 mm × 16 mm and with 2 mm notch were measured at a speed of 0.05 mm/min.

## III. Results and discussion

3.1. X-ray diffraction patterns

Figure 1a shows XRD patterns of the Ta_2AlC synthesized by SHS and PLS, exhibiting the presence of typical peaks of Ta_2AlC, TaC and Al_2O_3 for the sample prepared by SHS. The appearance of binary carbide, TaC indicates that the rapid reaction process involved in SHS leads to an insufficient reaction. At the same time, high temperature reaction of SHS can lead to Al oxidation. After removal of Al_2O_3, subjecting the sample to PLS method at 1500 °C for 1 h, phase pure Ta_2AlC could be obtained, reflecting that the binary carbide TaC can be completely converted into ternary carbides by further reaction.

Ta_4AlC_3 can be synthesized at 1500 °C using the phase pure Ta_2AlC and TaC powders with molar ratios

of Ta_2AlC : TaC = 1 : 0.8, 1 : 1.2, 1 : 1.6 and 1 : 1.8, as shown in Fig. 1b. Thus, finally the formation of Ta_4AlC_3 can be carried out according to the following reaction:

$$Ta_2AlC_{(s)} + TaC_{(s)} \longrightarrow Ta_4AlC_{3(s)} \qquad (1)$$
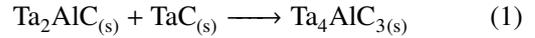
This indicates that the 413 ternary $M_{n+1}AX_n$ can also be synthesized by the reaction between 211 ternary $M_{n+1}AX_n$ and binary carbide MX, when previously the 312 ternary $M_{n+1}AX_n$ was obtained from the 211 ternary $M_{n+1}AX_n$ and binary carbide MX. For the different ratios of Ta_2AlC : TaC, phase pure Ta_4AlC_3 could be synthesized while the ratio of Ta_2AlC : TaC = 1 : 1.2 provided the formula $Ta_4Al_{1.25}C_{2.75}$, as presented in Table 1. Correspondingly, the deficiency of TaC leads to the incomplete transformation reaction and excess carbides become redundant. In this case, the excess of Al element and the lack of proportional carbon element are common phenomena in the synthesis of ternary ceramics.

Figure 1b shows the peaks for the Ta_4AlC_3 phase exhibiting that the (*hkl*) = (106) with $I_{observed}$ = 100% at 2θ of ~40.30°. These results are for the Ta_4AlC_3 powders, if only considering the relationship between Ta_4AlC_3 index and 2θ. Moreover, these results are also consistent with the previous reports [40,41]. When considering the 2θ and $I_{observed}$ = 100% of Ta_4AlC_3, the results are consistent with the examples in previous report [41]. The lattice parameters for the Ta_4AlC_3 obtained by PLS method are in the range of a = 3.1103–3.1157 Å, c = 23.9316–24.1670 Å, respectively. The lattice parameters a and c are higher than those of Ta_2AlC.

Furthermore, XRD patterns of the sample prepared by SPS at 1500 °C for 10 min with a heating rate of 80 °C/min and under a pressure of 30 MPa, using Ta_2AlC : TaC = 1 : 1.2 as raw materials were also obtained. Similar to the PLS samples, phase-pure bulk Ta_4AlC_3 was also found, as shown in Fig. 2. Extra phase transition was not found during the processing, indicating the occurrence of the same reaction as Eq. 1. How-
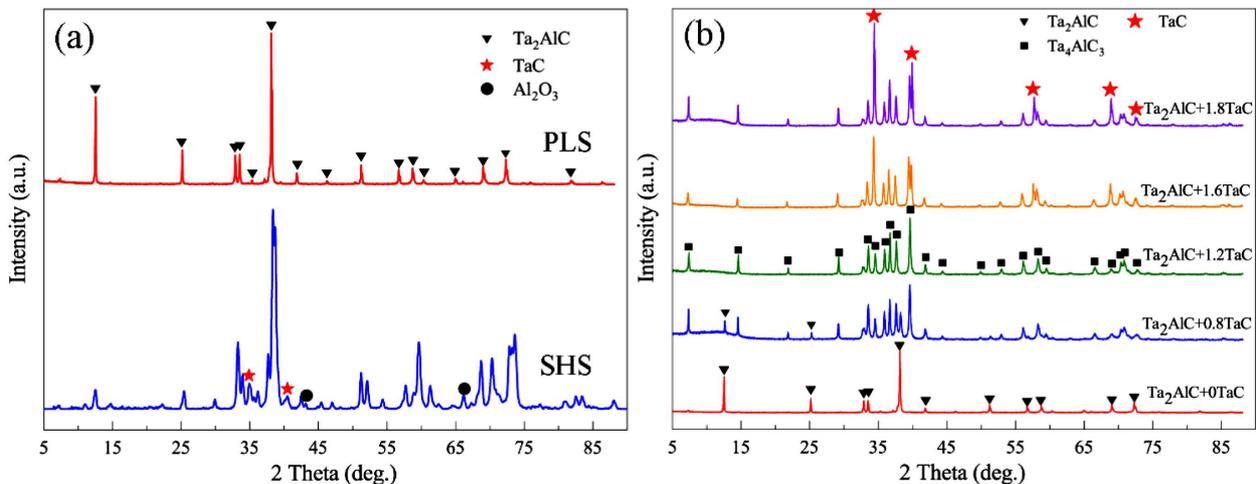

Figure 1. XRD patterns of the synthesized: a) Ta$_2$AlC and b) Ta$_4$AlC$_3$

Table 1. Summary of fabricated Ta-Al-C MAX phases reported in the literature and measured in this study (TS)

Raw material / Method	Formula	Phase	Parameters [Å]	Refs.
Ta : Al : C (carbon black) = 2 : 1.4 : 1 SHS	$Ta_2Al_{1.4}C$	Ta_2AlC, TaC and Al_2O_3	Ta_2AlC ($a = 3.0990 \pm 0.1223$, $c = 14.1338 \pm 0.0793$), $R_{wp} = 13.2\%$	TS
Ta : Al : C (carbon black) = 2 : 1.4 : 1 SHS + removal of Al_2O_3 + PLS	$Ta_2Al_{1.4}C$	Ta_2AlC	Ta_2AlC ($a = 3.0731 \pm 0.0039$, $c = 13.7685 \pm 0.0224$), $R_{wp} = 11.7\%$	TS
Ta_2AlC : TaC = 1 : 0.8 PLS	$Ta_4Al_{1.43}C_{2.57}$	Ta_2AlC Ta_4AlC_3	Ta_2AlC ($a = 3.0862 \pm 0.0039$, $c = 13.8211 \pm 0.0348$) Ta_4AlC_3 ($a = 3.1103 \pm 0.0007$, $c = 23.9750 \pm 0.0650$), $R_{wp} = 8.42\%$	TS
Ta_2AlC : TaC = 1 : 1.2 PLS	$Ta_4Al_{1.25}C_{2.75}$	Ta_4AlC_3	Ta_4AlC_3 ($a = 3.1157 \pm 0.0018$, $c = 23.9316 \pm 0.1180$), $R_{wp} = 9.40\%$	TS
Ta_2AlC : TaC = 1 : 1.6 PLS	$Ta_4Al_{1.11}C_{2.89}$	Ta_4AlC_3, TaC	Ta_4AlC_3 ($a = 3.1149 \pm 0.0028$, $c = 24.1670 \pm 0.0243$), $R_{wp} = 11.70\%$	TS
Ta_2AlC : TaC = 1 : 1.8 PLS	$Ta_4Al_{1.05}C_{2.95}$	Ta_4AlC_3, TaC	Ta_4AlC_3 ($a = 3.1075 \pm 0.0006$, $c = 23.9933 \pm 0.0915$), $R_{wp} = 7.96\%$	TS
Ta_2AlC : TaC = 1 : 1.2 SPS	$Ta_4Al_{1.25}C_{2.75}$	Ta_4AlC_3	Ta_4AlC_3 ($a = 3.1080 \pm 0.0013$, $c = 24.0567 \pm 0.0145$), $R_{wp} = 5.53\%$	TS
Ta_2AlC : TaC = 1 : 1.2 SPS + HT 1 h	$Ta_4Al_{1.25}C_{2.75}$	Ta_4AlC_3	Ta_4AlC_3 ($a = 3.1098 \pm 0.0015$, $c = 24.0809 \pm 0.0298$), $R_{wp} = 12.94\%$	TS
Ta_2AlC : TaC = 1 : 1.2 SPS + HT 2 h	$Ta_4Al_{1.25}C_{2.75}$	Ta_4AlC_3	Ta_4AlC_3 ($a = 3.1160 \pm 0.0013$, $c = 24.1697 \pm 0.0444$), $R_{wp} = 12.63\%$	TS
Ta_2AlC : TaC = 1 : 1.2 SPS + HT 4 h	$Ta_4Al_{1.25}C_{2.75}$	Ta_4AlC_3	Ta_4AlC_3 ($a = 3.1267 \pm 0.0034$, $c = 24.1720 \pm 0.0039$), $R_{wp} = 8.81\%$	TS
Ta_2AlC : TaC = 1 : 1.2 SPS + HT 8 h	$Ta_4Al_{1.25}C_{2.75}$	Ta_4AlC_3	Ta_4AlC_3 ($a = 3.1331 \pm 0.0293$, $c = 24.1753 \pm 0.0068$), $R_{wp} = 13.86\%$	TS
Ta : Al : C(graphite) = 2 : 1.2 : 0.9 HP	$Ta_2Al_{1.2}C_{0.9}$	Ta_2AlC	Ta_2AlC ($a = 3.081$ Å, $c = 13.89$ Å)	[44]
Ta : Al : C(graphite) = 2 : 1.2 : 0.9 HP	$Ta_2Al_{1.2}C_{0.9}$	Ta_2AlC	Ta_2AlC ($a = 3.079$ Å, $c = 13.854$ Å)	[45]
Ta : Al : C(graphite) HP	-	Ta_4AlC_3	Ta_4AlC_3 ($a = 3.0916$ Å, $c = 23.7078$ Å)	[40]
Ta : Al : C(graphite) HP	-	Ta_4AlC_3	Ta_4AlC_3 ($a = 3.0918$ Å, $c = 23.7082$ Å)	[35]
Ta_2H : Al : C(graphite) = 2 : 1.25 : 2.6 SPS	$Ta_4Al_{1.25}C_{2.6}$	α-Ta_4AlC_3 β-Ta_4AlC_3	α-Ta_4AlC_3 ($a = 3.133(6)$ Å, $c = 24.10(9)$ Å) β-Ta_4AlC_3 ($a = 3.086(5)$ Å, $c = 23.74(1)$ Å)	[41]

ever, compared to the powder XRD results of Ta_4AlC_3 obtained by the PLS method, the relative intensity of diffraction peaks exhibited obvious preferential growth orientation due to the high pressure in the SPS processing. Thus, the main crystal plane $(hkl) = (0010)$ with $I_{observed} = 100\%$ at 2θ of ~37.50° was observed, which is consistent with the previously reported bulk Ta_4AlC_3 samples prepared by HP and SPS [41]. However, the lattice parameters a and c are comparable with those of the PLS samples as well as the results in previous literature reports [41]. The lattice parameters for the Ta_4AlC_3 sample obtained by SPS and subsequent HT are in the range of $a = 3.1080$–3.1331 Å and $c = 23.9933$–24.1753 Å, respectively. The lattice parameters a and c increase with increasing heat treatment time of the SPS sintered sample at 1500 °C from 0 to 8 h, which may be attributed to stress release and grain growth of bulk

Ta_4AlC_3 at elevated temperature of 1500 °C. However, no obvious phase change was observed in the bulk sample, indicating that the bulk Ta_4AlC_3 at 1500 °C is relatively stable.

3.2. Microstructure

Figure 3a shows typical SEM micrographs of the fractured surface of the as-sintered bulk Ta_4AlC_3 sample by SPS, exhibiting the existence of typical laminated structure at the cleavage planes. The average length of the large Ta_4AlC_3 grains prepared by SPS at 1500 °C as measured to be 4.92 ± 0.11 μm. A large number of ~1 μm fine grains and several fine pores could also be observed. After heat treatment at 1500 °C for 2, 4 and 8 h, fine grains and pores disappeared and the average grain sizes of the grains gradually increased. It is thus indicated that coarse grains tend to form and grow in the
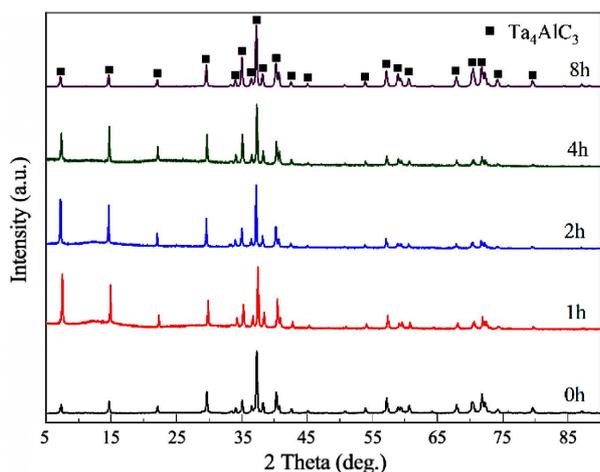
Figure 2. XRD patterns of Ta$_4$AlC$_3$ fabricated by SPS of the sample Ta$_2$AlC : TaC = 1 : 1.2 and heat treated at 1500 °C under different time

Ta$_4$AlC$_3$ in the process of heat treatment temperature of 1500 °C. However, the grain size of the bulk Ta$_4$AlC$_3$ prepared by SPS and heat treated at 1500 °C for 8 h was 7.61 ± 0.14 μm, which is still smaller than that of the bulk Ta$_4$AlC$_3$ obtained by HP at 1500 °C for 1 h. All in all, the rapid synthesis method of SPS is propitious to fabricate fine grain size M$_{n+1}$AX$_n$ phase.

3.3. Mechanical properties

Figure 4 illustrates the effect of heat treatment on the Vickers hardness of the bulk Ta$_4$AlC$_3$ sintered by SPS. Clearly, the hardness of the Ta$_4$AlC$_3$ decreases gradually with the increase of heat treatment time. Further-

more, the grain sizes of the Ta$_4$AlC$_3$, exhibit an increasing tendency with increasing heat treatment time. This reflects that the fine grain size of the Ta$_4$AlC$_3$ results in higher microhardness, i.e. Vickers hardness.

The variation of densities of the bulk Ta$_4$AlC$_3$ ceramics after different heat treatment times is shown in Fig. 5. With increasing heat treatment time from 0 to 8 h, the density changes from 11.636 to 12.165 g/cm^3. Correspondingly, the relative density increases from 90.7 to 94.2% TD. Consequently, the growth of grains during heat treatment can lead to the disappearance of pores and the increase of density, which was also indicated by the microstructure observation.

Effect of heat treatment times on the flexural strength and the fracture toughness of bulk Ta$_4$AlC$_3$ prepared
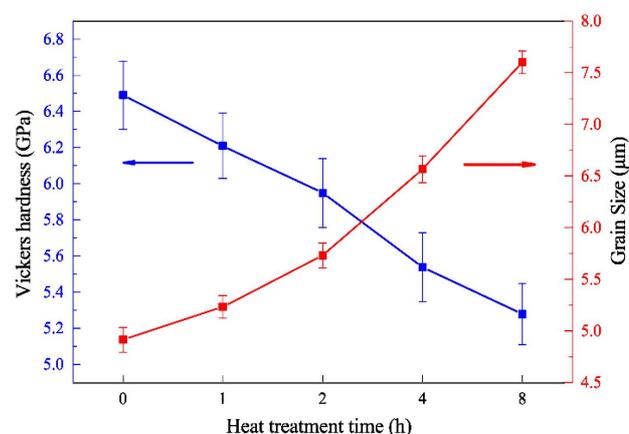

Figure 4. Effect of heat treatment time on the Vickers hardness of bulk Ta$_4$AlC$_3$ fabricated by SPS
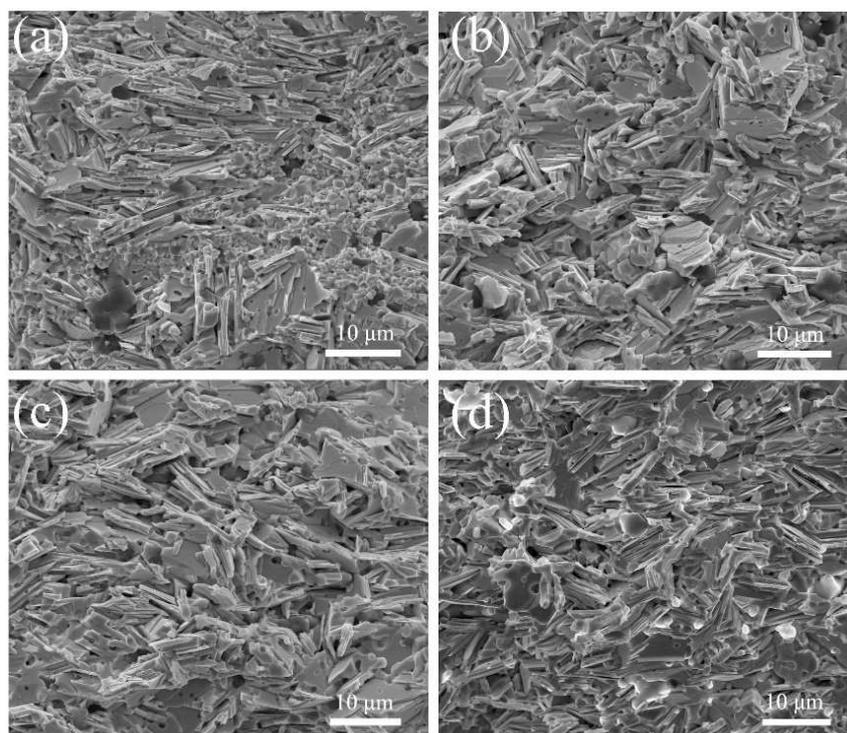

Figure 3. SEM images of fractured surfaces of Ta$_4$AlC$_3$ fabricated by SPS and heat treated at 1500 °C for: a) 0 h, b) 2 h, c) 4 h, and d) 8 h
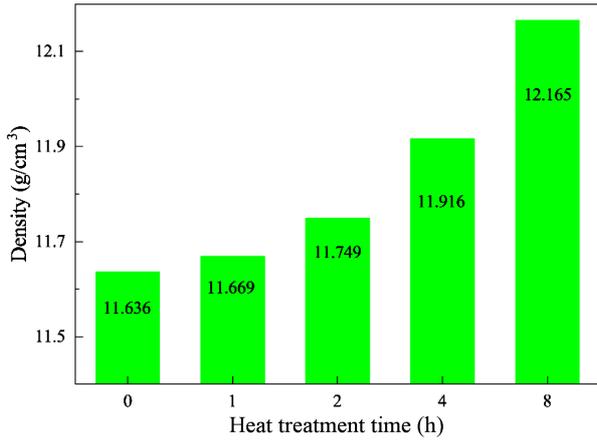
Figure 5. Variation of density of bulk Ta_4AlC_3 ceramics with different heat treatment time

by SPS is shown in Figs. 6a and 6b, respectively. For the bulk Ta_4AlC_3 fabricated by SPS at 1500 °C for 10 min, the flexural strength and fracture toughness are 411 MPa and 7.11 MPa·m$^{1/2}$, respectively. The flexural strength is higher than those of the hot pressed MAX samples reported in the literature, i.e. Ta_4AlC_3 372 MPa [40], Ta_4AlC_3 407 MPa [41], Nb_4AlC_3 346 MPa [46] and Ta_2AlC 360 MPa [45]. However, the fracture tough-

ness is comparable to that of the hot pressed samples, namely, Ta_4AlC_3 7.7 MPa·m$^{1/2}$ [40], Ta_4AlC_3 5.0 MPa·m$^{1/2}$ [41], Nb_4AlC_3 7.1 MPa·m$^{1/2}$ [46] and Ta_2AlC 7.7 MPa·m$^{1/2}$ [45]. Summary of fabrication methods and mechanical properties compared to previous studies on bulk Ta_4AlC_3, Nb_4AlC_3 and Ta_2AlC is presented in Table 2.

IV. Conclusions

Bulk, dense and phase-pure Ta_4AlC_3 ceramics were fabricated by SPS via powders metallurgical route involving solid-solid reaction of Ta_2AlC and TaC. By regulating the Ta_2AlC and TaC stoichiometric ratio, the reaction was achievable during the preparation process. Phase-pure Ta_4AlC_3 ceramics were fabricated by SPS using mixtures with molar ratio of Ta_2AlC : TaC = 1 : 1.2 at 1500 °C for 10 min under a pressure of 30 MPa. The molar ratio of Ta_2AlC : TaC = 1 : 1.2 also proved to be a valid mixture for the PLS Ta_4AlC_3 powders at 1500 °C for 1 h. Contradicting results reported previously in the literature were resolved, thus the XRD peak $I_{observed}$ = 100% of Ta_4AlC_3 was obtained for crystal plane (hkl) = (106) at 2θ of ~40.30° or at (hkl) = (0010) at 2θ of ~37.50° depending on the processing method. The density, Vickers hardness, flexural strength
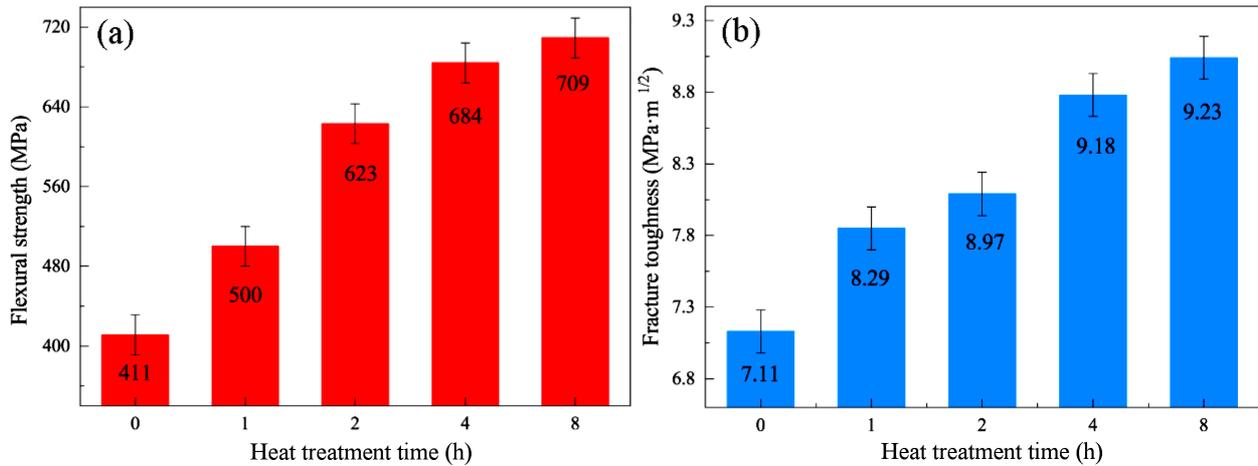

Figure 6. Variation of flexural strength and fracture toughness of bulk Ta_4AlC_3 ceramics with different heat treatment time: a) flexural strength and b) fracture toughness

Table 2. Summaries of the fabrication methods, density (ρ) and mechanical properties (Vickers hardness *HV*, fracture toughness K_{IC} and flexural strength σ) of bulk Ta_4AlC_3, Nb_4AlC_3 and Ta_2AlC reported in the literature and measured in this study (TS)

Phase	Raw material / Method	ρ [g/cm³]	*HV* [GPa]	K_{IC} [MPa·m$^{1/2}$]	σ [MPa]	Refs.
Ta_4AlC_3	Ta_2AlC and TaC / SPS	11.64	5.28	7.11	411	TS
Ta_4AlC_3	Ta_2AlC and TaC / SPS + HT 1 h	11.67	5.54	8.29	500	TS
Ta_4AlC_3	Ta_2AlC and TaC / SPS + HT 2 h	11.75	5.95	8.97	623	TS
Ta_4AlC_3	Ta_2AlC and TaC / SPS + HT 4 h	11.92	6.21	9.18	684	TS
Ta_4AlC_3	Ta_2AlC and TaC / SPS + HT 8 h	12.17	6.49	9.23	709	TS
Ta_4AlC_3	Ta, Al and C / HP	13.18	5.1	7.7	372	[40]
Ta_4AlC_3	Ta_2H, Al and C / HP	12.27	6.1	5.0	407	[41]
Nb_4AlC_3	Nb, Al and C / HP	6.97	2.6	7.1	346	[46]
Ta_2AlC	Ta, Al and C / HP	11.46	-	7.7	360	[45]

and fracture toughness of the bulk Ta_4AlC_3 ceramics were found to be $11.64\,g/cm^3$, $5.28\,GPa$, $411\,MPa$ and $7.11\,MPa\cdot m^{1/2}$, respectively. The bulk Ta_4AlC_3 heat treated at elevated temperature of $1500\,°C$ was relatively stable even for the dwell time of 8 h. However, the growth of fine grains of the Ta_4AlC_3 fabricated by SPS during the heat treatment could lead to the disappearance of pores and the increase of density, which also resulted in the significant increase in the flexural strength and the fracture toughness of bulk Ta_4AlC_3 ceramics.

References

1. M.W. Barsoum, "The $M_{n+1}AX_n$ phases: A new class of solids", *Prog. Solid State Chem.*, **28** [1-4] (2000) 201–281.

2. J.C. Schuster, H. Nowotny, C. Vaccaro, "The ternary systems: CrAlC, VAlC, and TiAlC and the behavior of H-phases (M_2AlC)", *J. Solid State Chem.*, **32** [2] (1980) 213–219.

3. W. Jeitschko, H. Nowotny, "Die Kristallstruktur von Ti_3SiC_2 ein neuer Komplexcarbid-Typ", *Monatshefte Chemie.*, **98** [2] (1967) 329–337.

4. H. Wolfsgruber, H. Nowotny, F. Benesovsky. "Die Kristallstruktur von Ti_3GeC_2", *Monatshefte Chemie.*, **98** [6] (1967) 2403–2405.

5. H. Nowotny, "Strukturchemie einiger Verbindungen der Übergangsmetalle mit den elementen C, Si, Ge, Sn", *Prog. Solid State Chem.*, **5** (1971) 27–70.

6. M. Sokol, N. Varun, K. Sankalp, M.W. Barsoum, "On the chemical diversity of the MAX phases", *Trends. Chem.*, **1** [2] (2019) 210–223.

7. M.W. Barsoum, E.R. Tamer, "Synthesis and characterization of a remarkable ceramic: Ti_3SiC_2", *J. Am. Ceram. Soc.*, **79** [7] (1996) 1371–1378.

8. Y.C. Zhou, Z.M. Sun, S.Q. Chen, Y. Zhang, "In-situ hot pressing/solid-liquid reaction synthesis of dense titanium silicon carbide bulk ceramics", *Mater. Res. Innov.*, **2** [3] (1998) 142–146.

9. P. Eklund, J.-P. Palmquist, J. Hoewing, D.H. Trinh, E.-R. Tamer, H. Högberg, L. Hultman, "Ta_4AlC_3: Phase determination, polymorphism and deformation", *Acta Mater.*, **55** [14] (2007) 4723–4729.

10. P. Eklund, J. Rosen, P.O.Å. Persson, "Layered ternary $M_{n+1}AX_n$ phases and their 2D derivative MXene: An overview from a thin-film perspective", *J. Phys. D Appl. Phys.*, **50** [11] (2017) 113001.

11. T. Yang, Q.Y. Chen, X.H. Li, C.M. Meng, B. Ye, B.B. Gou, "Low-temperature synthesis of $Ti_3Al(Sn)C_2$ solid solution using replacement reaction", *J. Mater. Sci. Mater. Electron.*, **31** (2020) 20601–20610.

12. L. Qu, G. Bei, B. Stelzer, H. Rueß, J.M. Schneider, D. Cao, S. der Zwaag, W.G. Sloof, "Synthesis, crystal structure, microstructure and mechanical properties of $(Ti_{1-x}Zr_x)_3SiC_2$ MAX phase solid solutions", *Ceram. Int.*, **45** [1] (2019) 1400–1408.

13. H.L. Gao, R. Benitez, W. Son, R. Arroyave, M. Radovic, "Structural, physical and mechanical properties of $Ti_3(Al_{1-x}Si_x)C_2$ solid solution with x = 0–1", *Mater. Sci. Eng. A*, **676** [31] (2016) 197–208.

14. Z.M. Liu, L.Y. Zheng, L.C. Sun, Y.H. Qian, J.Y. Wang, M.S. Li, "($Cr_{2/3}Ti_{1/3})_3$AlC$_2$ and ($Cr_{5/8}Ti_{3/8})_4$AlC$_3$: New MAX-phase compounds in Ti-Cr-Al-C system", *J. Am. Ceram. Soc.*, **97** [1] (2014) 67–69.

15. T. Cabioc'h, P. Eklund, V. Mauchamp, M. Jaouen, "Structural investigation of substoichiometry and solid solution effects in $Ti_2Al(C_x,N_{1-x})_y$ compounds", *J. Eur. Ceram. Soc.*, **32** [8] (2012) 1803–1811.

16. M. Radovic, A. Ganguly, M.W. Barsoum, "Elastic properties and phonon conductivities of $Ti_3Al(C_{0.5},N_{0.5})_2$ and $Ti_2Al(C_{0.5},N_{0.5})$ solid solutions", *J. Mater. Res.*, **23** [6] (2008) 1517–1521.

17. G.B. Ying, F.C. Ma, L. Su, X.D. He, C. Zhang, Z.H. Dai, H. Luo, S.Y. Du, C. Wang, "An ab initio prediction study of the electronic structure and elastic properties of V_3GeC_2", *Process. Appl. Ceram.*, **11** [2] (2017) 82–86.

18. G.B. Ying, X.D. He, M.W. Li, W.B. Han, F. He, S.Y. Du, "Synthesis and mechanical properties of high-purity Cr_2AlC ceramic", *Mater. Sci. Eng. A*, **528** [6] (2011) 2635–2640.

19. M. Radovic, M.W. Barsoum, "MAX phases: bridging the gap between metals and ceramics", *Am. Ceram. Soc. Bull.*, **92** [3] (2013) 20–27.

20. M. Naguib, M. Kurtoglu, V. Presser, J. Lu, J.J. Niu, M. Heon, L. Hultman, Y. Gogotsi, M.W. Barsoum, "Two-dimensional nanocrystals produced by exfoliation of Ti_3AlC_2", *Adv. Mater.*, **23** [37] (2011) 4248–4253.

21. R. Syamsai, A.N. Grace, "Ta_4C_3 MXene as supercapacitor electrodes", *J. Alloy. Compd.*, **792** [5] (2019) 1230–1238.

22. H. Li, X. Wang, H. Li, S. Lin, B.C. Zhao, J.M. Dai, W.H. Song, X.B. Zhu, Y.P. Sun, "Capacitance improvements of $V_4C_3T_x$ by NH_3 annealing", *J. Alloy. Compd.*, **784** (2019) 923–930.

23. S.S Zhao, C.F. Chen, X. Zhao, X.F. Chu, F. Du, G. Chen, Y. Gogotsi, Y. Gao, Y. Dall'Agnese, "Flexible $Nb_4C_3T_x$ film with large interlayer spacing for high-performance supercapacitors", *Adv. Funct. Mater.*, **30** [47] (2020) 2000815.

24. X.H. Chen, G.P. Bei, "Toughening mechanisms in nanolayered max phase ceramics - A review", *Materials*, **10** [4] (2017) 366.

25. M.W. Barsoum, R. Miladin, "Elastic and mechanical properties of the MAX phases", *Annu. Rev. Mater. Res.*, **41** (2011) 195–227.

26. A.-S. Farlea, C. Kwakernaak, S.V.D. Zwaag, W.G. Sloof, "A conceptual study into the potential of $M_{n+1}AX_n$-phase ceramics for self-healing of crack damage", *J. Eur. Ceram. Soc.*, **35** [1] (2015) 37–45.

27. M.W. Barsoum, E.-R. Tamer, "The MAX phases: Unique new carbide and nitride materials", *Am. Sci.*, **89** [4] (2001) 334–343.

28. M.W. Barsoum, G.J. Tucker, "Deformation of layered solids: Ripplocations not basal dislocations", *Scripta Mater.*, **139** (2017) 166–172.

29. L. Liu, G.B. Ying, C. Hu, K.C. Zhang, F.C. Ma, L. Su, C. Zhang, C. Wang, "Functionalization with MXene (Ti_3C_2) enhances the wettability and shear strength of carbon fiber-epoxy composites", *ACS Appl. Nano Mater.*, **2** [9] (2019) 5553–5562.

30. L. Su, G.B. Ying, L. Liu, F.C. Ma, K.C. Zhang, C. Zhang, X. Wang, C. Wang, "$Ti_3C_2T_x$ on copper and nickel foams

with improved electrochemical performance produced via solution processing for supercapacitor", *Process. Appl. Ceram.*, **12** [4] (2018) 366–373.

31. L.F. Gao, C. Li, W.C. Huang, S. Mei, H. Lin, Q. Ou, Y. Zhang, J. Guo, F. Zhang, S.X. Xu, "MXene/polymer membranes: Synthesis, properties, and emerging applications", *Chem. Mater.*, **32** [5] (2020) 1703–1747.

32. A.T. Zhang, R. Liu, J.M. Tian, W.G. Huang, J.Q. Liu, "MXene-based nanocomposites for energy conversion and storage applications", *Chem. Eur. J.*, **26** [29] (2020) 6342–6359.

33. G.B. Ying, A.D. Dillon, A.T. Fafarman, M.W. Barsoum, "Transparent, conductive solution processed spincast 2D Ti_2CT_x (MXene) films", *Mater. Res. Lett.*, **5** [6] (2017) 391–398.

34. L. Liu, G.B. Ying, D. Wen, K.C. Zhang, C. Hu, Y.T. Zheng, C. Zhang, X. Wang, C. Wang, "Aqueous solution-processed MXene ($Ti_3C_2T_x$) for non-hydrophilic epoxy resin-based composites with enhanced mechanical and physical properties", *Mater. Design*, **197** (2021) 109276.

35. Z.J. Lin, M.J. Zhuo, Y.C. Zhou, M.S. Li, J.Y. Wang, "Structural characterization of a new layered-ternary Ta_4AlC_3 ceramic", *J. Mater. Res.*, **21** [10] (2006) 2587–2592.

36. B. Manoun, S.K. Saxena, "High-pressure X-ray diffraction study of Ta_4AlC_3", *Appl. Phys. Lett.*, **88** [20] (2006) 201902.

37. Y.L. Du, Z.M. Sun, H. Hashimoto, W.B. Tian, "First-principles study of polymorphism in Ta_4AlC_3", *Solid State Commun.*, **145** [9-10] (2008) 461–464.

38. M. Dahlqvist, A. Thore, J. Rosen, "Electronic structure, bonding characteristics, and mechanical properties in $(W_{2/3}Sc_{1/3})_2AlC$ and $(W_{2/3}Y_{1/3})_2AlC$ i-MAX phases from first-principles calculations", *J. Phys. Condens. Matter*, **30** [30] (2018) 305502.

39. M. Dahlqvist, J. Lu, R. Meshkian, Q.Z. Tao, L. Hultman, J. Rosen, "Prediction and synthesis of a family of atomic laminate phases with Kagomé-like and in-plane chemical ordering", *Sci. Adv.*, **3** [7] (2017) e1700642.

40. C.F. Hu, Z.J. Lin, L.F. He, Y.W. Bao, J.Y. Wang, M.S. Li, Y.C. Zhou , "Physical and mechanical properties of bulk Ta_4AlC_3 ceramic prepared by an in situ reaction synthesis/hot-pressing method", *J. Am. Ceram. Soc.*, **90** [8] (2007) 2542–2548.

41. M. Griseri, B. Tunca, T. Lapauw, S.G. Huang, L. Popescu, M.W. Barsoum, K. Lambrinou, J. Vleugels, "Synthesis, properties and thermal decomposition of the Ta_4AlC_3 MAX phase", *J. Eur. Ceram. Soc.*, **39** [10] (2019) 2973–2981.

42. C.L. Yeh, Y.S. Chen, "Effects of Al content on formation of TaC, Ta_2C, and Ta_2AlC by combustion synthesis with aluminothermic reactions", *Ceram. Int.*, **43** [17] (2017) 15659–15665.

43. T. Ramkumar, M. Selvakumar, R. Vasanthsankar, A.S. Sathishkumar, P. Narayanasamy, G. Girija, "Rietveld refinement of powders X-ray diffraction, microstructural and mechanical studies of magnesium matrix composites processed by high energy ball milling", *J. Magnesium Alloys*, **6** [4] (2018) 390–398.

44. C.F. Hu, J. Zhang, Y.W. Bao, J.Y. Wang, M.S. Li, Y.C. Zhou, "In-situ reaction synthesis and decomposition of Ta_2AlC", *Int. J. Mater. Res.*, **99** [1] (2008) 8–13.

45. C.F. Hu, L.F. He, J. Zhang, Y.W. Bao, J.Y. Wang, M.S. Li, Y.C. Zhou, "Microstructure and properties of bulk Ta_2AlC ceramic synthesized by an in situ reaction/hot pressing method", *J. Eur. Ceram. Soc.*, **28** [8] (2008) 1679–1685.

46. C.F. Hu, F.Z. Li, L.F. He, M.Y. Liu, J. Zhang, J.M. Wang, Y.W. Bao, J.Y. Wang, Y.C. Zhou, "In situ reaction synthesis, electrical and thermal, and mechanical properties of Nb_4AlC_3", *J. Am. Ceram. Soc.*, **91** [7] (2008) 2258–2263.